



Characterization of archaeological waterlogged wooden objects exposed on the hyper-saline Dead Sea shore



Asaf Oron ^{a,*}, Nili Liphshitz ^b, Benjamin W. Held ^c, Ehud Galili ^d, Micha Klein ^a, Raphael Linker ^e, Robert A. Blanchette ^c

^a Department of Geography and Environmental Studies, University of Haifa, Mount Carmel, Haifa 3498838, Israel

^b Tel Aviv University Institute of Archaeology – the Botanical Laboratories, Ramat Aviv, 69978 Tel Aviv, Israel

^c Department of Plant Pathology, University of Minnesota, St. Paul, MN 55108, USA

^d Israel Antiquities Authority and Zinman Institute of Archaeology, University of Haifa, POB 180, Atlit 30300, Israel

^e Faculty of Civil and Environmental Engineering, Technion-Israel Institute of Technology, Haifa 32000, Israel

ARTICLE INFO

Article history:

Received 22 March 2016

Received in revised form 16 June 2016

Accepted 27 June 2016

Available online xxxx

Keywords:

Dead Sea

Maritime activity

Waterlogged wood

Ancient driftwood

Hyper-saline environments

Wood deterioration

Conservation

ABSTRACT

Archaeological waterlogged wood objects exposed on the Dead Sea shore exhibit little visual evidence of degradation when first exposed, and after prolonged exposure and dehydration. An investigation on the state of preservation of this material was recognised as a necessary step towards its long-term conservation. Micromorphological observations, ATR FTIR, ash content, and physical tests showed that deterioration is limited and is mostly non-biological in nature. Natural bulking and impregnation with lake minerals and salts appear to play a significant role in the physical stability of these woods when dried, and apparently inhibit microbial colonization and subsequent degradation. In contrast, archaeological wood examined from a typical Mediterranean marine environment showed advanced stages of degradation by bacteria, with the wood structure extensively compromised.

© 2016 Elsevier Ltd. All rights reserved.

1. Introduction

The Dead Sea is a hyper-saline inland desert lake located at the lowest terrestrial place on Earth (Fig. 1). The lake and its surroundings have a harsh desert climate, extremely rugged terrain, and rich mineral resources.

The archaeological record of the Dead Sea basin is extremely long and diverse, indicating a continuous human presence at least from the Neolithic Period (9750–4500 BCE) to the present time (Nissenbaum, 1993; Taute, 1994; Gichon, 2000: 93–101; Recchi and Gopher, 2002; Hirschfeld, 2006; Barkai et al., 2007; Schaub and Chesson, 2007; Schyle, 2007; Vardi and Cohen-Sasson, 2012). This human presence was associated with the exploitation of the region's rich natural resources, e.g., salt, bitumen (natural asphalt), and flint, as well as the cultivation of dates and aromatic plants at several lakeshore oases.

A severe and ongoing drop in the lake water level since the 1960's (Klein, 1982; Bookman et al., 2006: 167–168) has led to the exposure of vast areas of the former lakebed, and with it a diverse collection of

ancient and historical objects. Of particular importance are several well preserved anchors made of stone, waterlogged wood and rope, dating from the 8th century BC to the 12th century AD (Hadas, 1992, 1993; Hadas et al., 2005; Oron et al., 2008). Together with cargo remains, shoreline finds and other types of evidence, these anchors add significantly to our knowledge of the basin's history and illuminate the lake's unique maritime cultural landscape (Oron et al., 2015a, 2015b).

Waterlogged wood finds from the Dead Sea may be found while still wet or damp near the waterline, or completely dry, having been exposed for several years, or even decades, such as the anchors in Fig. 2a and b. Both appear visually and physically intact, with their three-dimensional integrity little changed. This seemingly un-degraded condition is unusual, and contrasts with similar finds from other marine environments, which are normally found chemically and biologically degraded, and prone to rapid disintegration upon uncontrolled drying (Hoffmann and Jones, 1990; Blanchette and Hofmann, 1994; Gelbrich et al., 2008; Björdal, 2012).

The excellent state of preservation of wooden finds from the Dead Sea raises questions regarding their physical and chemical nature. The aim of the study was to characterize the deterioration found in archaeological waterlogged wooden objects and other waterlogged wood found in and along the shoreline of the Dead Sea, using protocols commonly used for the evaluation of archaeological waterlogged wood

* Corresponding author.

E-mail addresses: asaforo@gmail.com (A. Oron), nilili@post.tau.ac.il (N. Liphshitz), bheld@umn.edu (B.W. Held), udi@israantique.org.il (E. Galili), mklein@geo.haifa.ac.il (M. Klein), linkerr@tx.technion.ac.il (R. Linker), robertb@umn.edu (R.A. Blanchette).

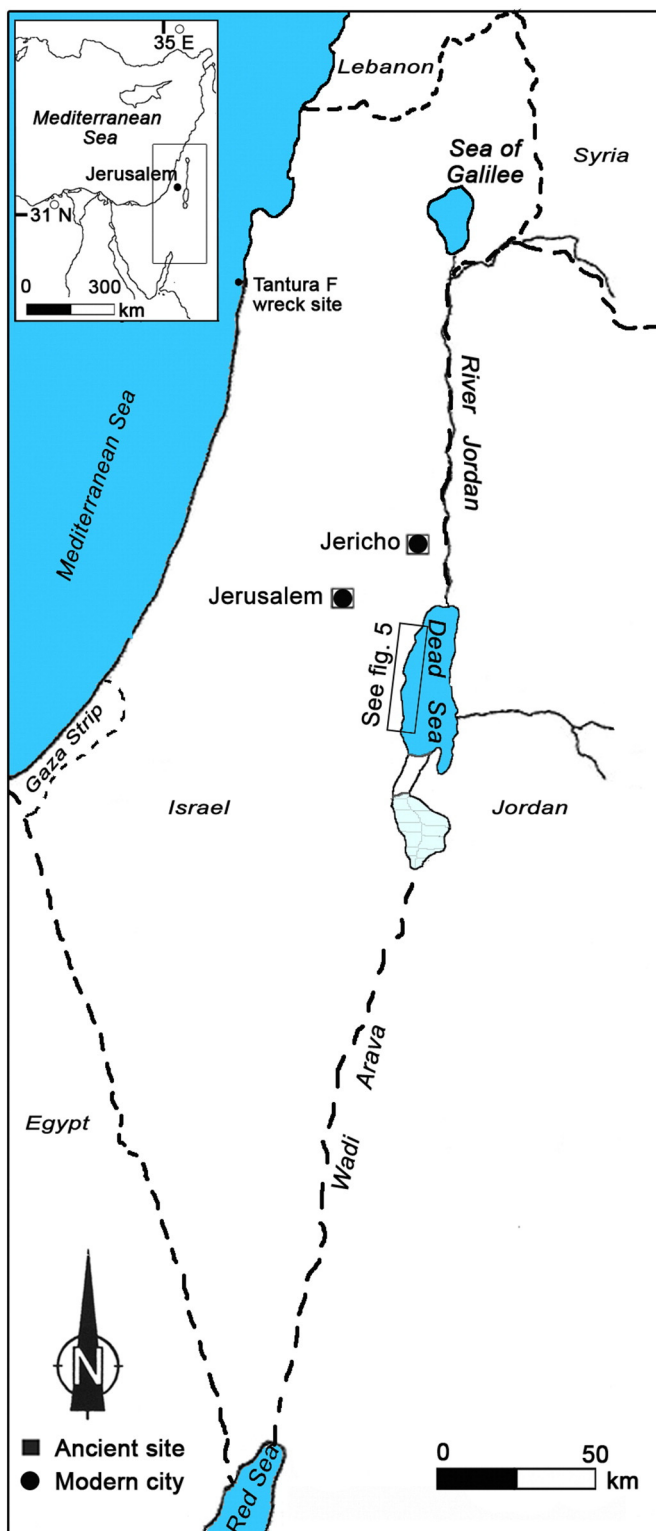


Fig. 1. Map of research area showing the eastern Mediterranean (inset) and the Dead Sea region (A. Oron).

material. This information is fundamental to the development of suitable long-term conservation methods for the lake's waterlogged wood cultural remains. For comparative purposes, waterlogged archaeological wood from the Late Byzantine Tantara F shipwreck found in the Mediterranean Sea (hereafter termed 'Tantara F') was also studied (Barkai and Kahanov, 2007; Barkai et al., 2010; Lipshitz, 2012).



Fig. 2. Composite anchors. a) Composite anchor (Anchor A, Oron et al., 2008, sample DS 8, ^{14}C dating: cal 898–1048 CE [97.9%]) made of stone, wood and rope as found still wet at the waterline. b) Composite anchor (Samar Springs anchor C, Oron et al., 2008, ^{14}C dating: cal 1032–1160 CE [100.0%]) made of stone, wood and rope as found fully dehydrated after several years of exposure (scale 20 cm, photos A. Oron).

2. Materials and methods

2.1. Study material

The rarity and intact nature of the archaeological wooden objects from the Dead Sea restricts their sampling to minute segments of wood suitable mainly for tree species analysis and density measurements. Data for the study were thus collected either in-situ directly from these objects when possible, or otherwise from readily available archaeological waterlogged driftwood found along the lake shore that could be destructively tested (Fig. 3). The latter originates from the densely forested banks of the Jordan River and from other freshwater sources around the lake (Zohary, 1962: 144–152, 165–177). Its presence in the lake is linked with powerful flash floods common to the region, and from the erosion of the soft marl banks of the Jordan River, which result in the washing of large amounts of this vegetation into the lake every year. Waterlogged objects and driftwood finds exposed by the receding shoreline are often found heavily encrusted with layers of lake minerals (Fig. 4).

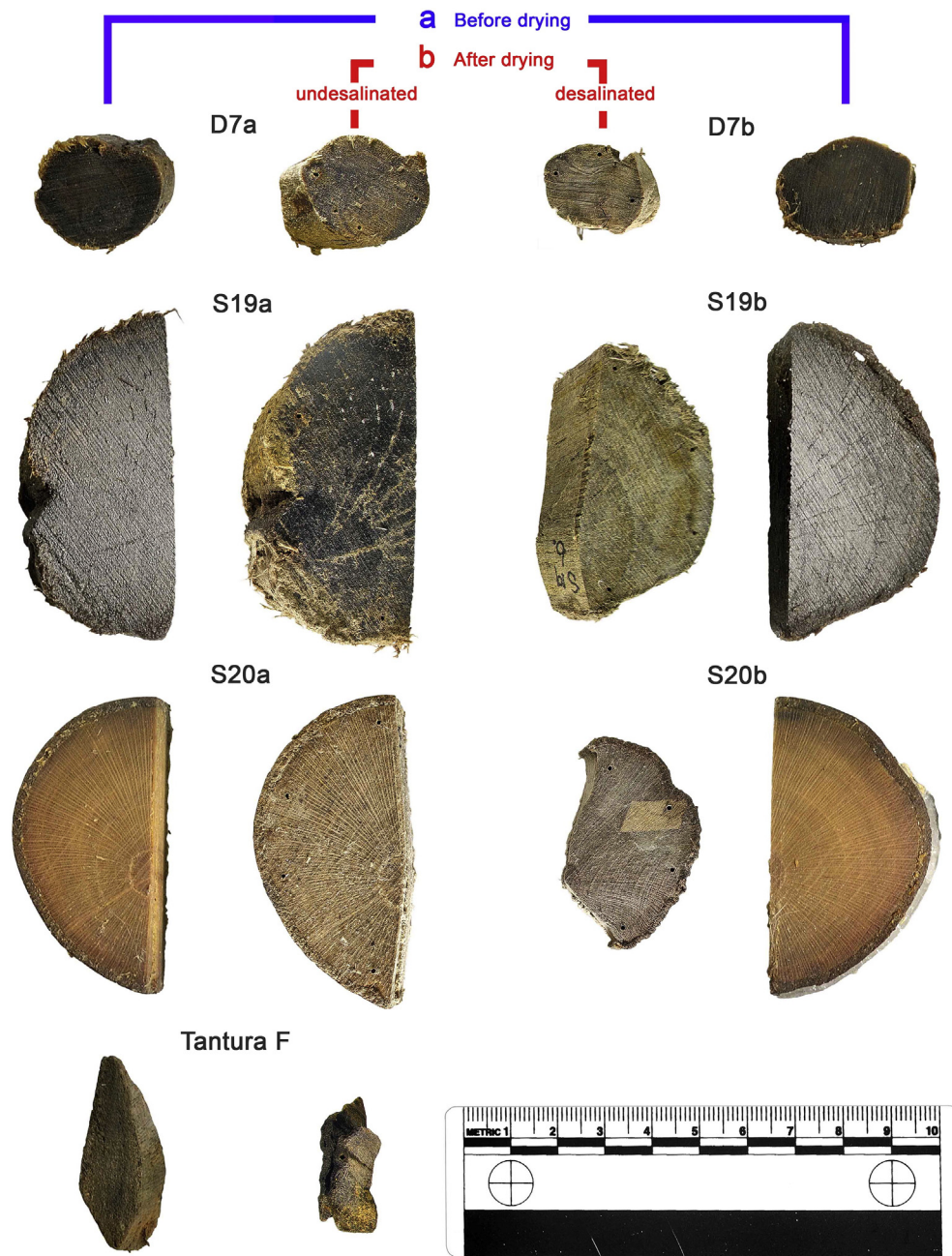


Fig. 3. Effects of air-drying on wooden objects. a) The wood samples before air-drying. b) The wood samples after slow air-drying: left – with their mineral content; right – without their soluble mineral content (photo A. Oron).

Eleven samples of waterlogged archaeological wood were collected for this study at several locations along the western shores of the lake's northern basin (Fig. 5).

Their dating was established by radiocarbon analysis (Table 1).

The research sample group from the Dead Sea was supplemented by a sample of a related tree species obtained from the Tantara F (Barkai and Kahanov, 2007; Barkai et al., 2010; Liphshitz, 2012, 5). Non-degraded modern wood samples of identical tree species were also collected within the research zone as references. Information about the different samples is summarized in Table 1.

The study material was subjected to wood species analysis, micro-morphological characterization, physical analysis, ash content measurements and ATR FTIR analysis.

2.2. Identification of wood species

Wood samples of 0.5–1 cm³ were taken from each wood piece for microscopic examination. Radial, longitudinal and tangential sections were prepared for each sample with a sharp razor blade. The species level identification of the samples was based on microscopic comparison between the three-dimensional structure of the wood and illustrations of anatomical characteristics of wood of modern trees and shrubs from reference books (Fahn et al., 1986; Schweingruber, 1990).

2.3. Micro-morphological characterization

Small segments of the wood samples from the Dead Sea and from the Tantara F were cut and prepared for scanning electron microscopy. Samples were infiltrated with TBS™ Tissue Freezing medium™

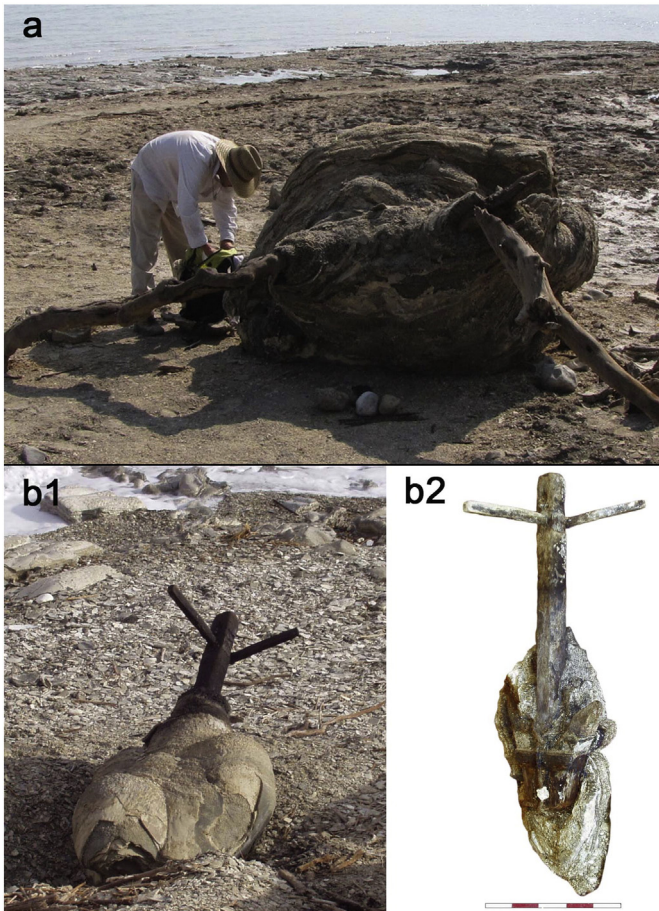


Fig. 4. Concretions of minerals on wooden finds. a) Ancient driftwood encased in a massive layer of minerals on the Dead Sea shore. b1) Roman anchor made of wood, lead and copper as found on the lakeshore encased in a thick layer of minerals (Hadas et al., 2005, ^{14}C dating: 2nd century BCE–1st century CE). b2) Roman anchor after partial cleaning (scale 50 cm, Photos G. Hadas).

(Triangle Biomedical Sciences, Durham, NC, USA) using low vacuum, mounted on brass stubs at $-20\text{ }^{\circ}\text{C}$ in an OM 2488 Minotome (International Equipment Company, Needham Heights, MA, USA), and cut to produce a transverse section of the wood segment. Samples were then thawed, air-dried for 48 h, mounted on stubs and coated with gold in an EMS 76M sputter coater (Ernest F. Fullam, Inc., Schenectady, NY, USA). Prepared samples were examined and digital photographs obtained using a Hitachi S3500N (Hitachi, Tokyo, Japan) scanning electron microscope.

2.4. Physical analysis

The physical analyses comprised maximum water content (MWC), basic density (D_b), residual basic density (RBD), loss of wood substance (LWS), linear shrinkage (β_t , β_r , β_l) cross-sectional shrinkage (β_{cs}) and Anti-Shrinkage Efficiency (ASE). The formulas used in these calculations are presented in Table 2, and the results in Table 3.

The sampling methods used in the physical analyses were adapted to the availability of original material and the inherent restriction of sampling intact cultural heritage material. Three sampling procedures were followed in order to collect as much information as possible within these restrictions (see Table 1 for the procedure used for each sample);

1) Small prismatic sections measuring 0.5–1.5 cm longitudinally, and 0.5 cm radially and tangentially, were used for samples from small driftwood stems and archaeological objects.

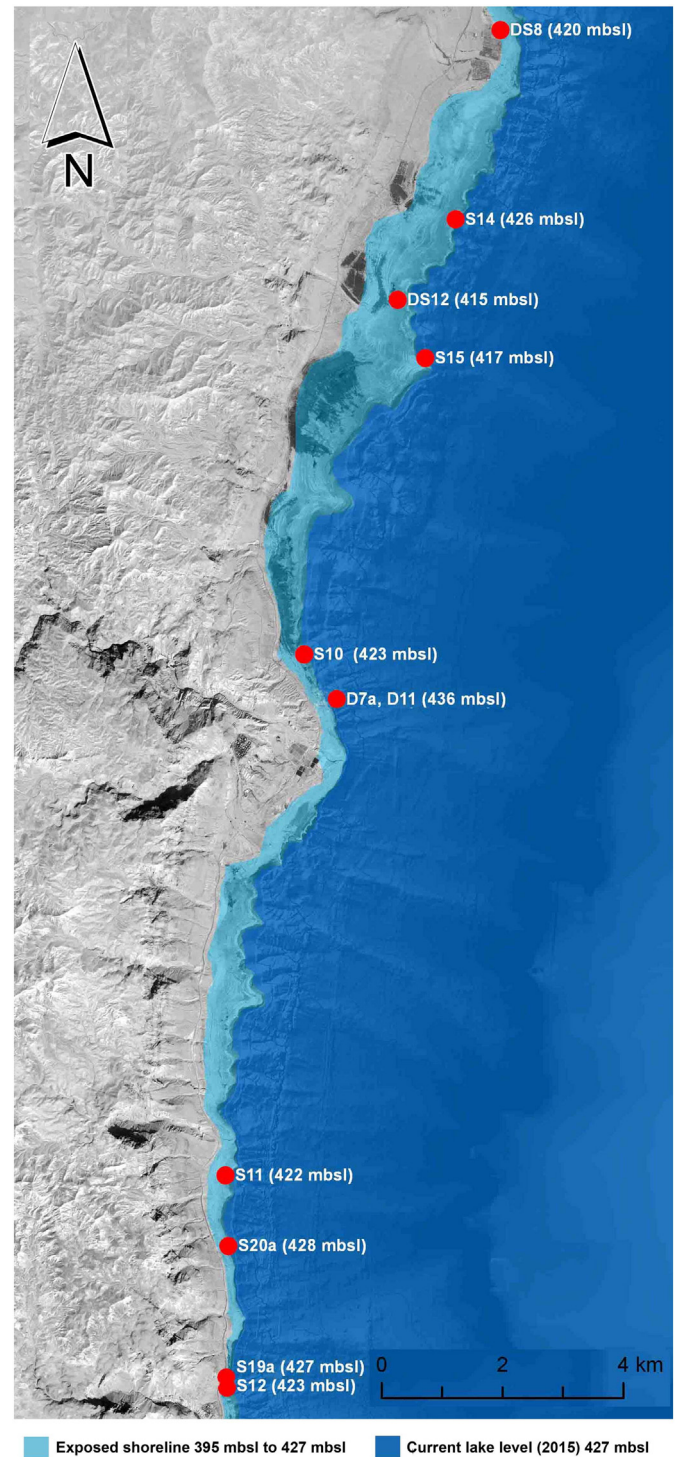


Fig. 5. Locations and elevations of the find places of wooden objects and driftwood sampled for the study. Elevations: Meters below sea level (mbsl ± 5 m accuracy). (GIS data superimposed on a modified multi-beam image of the lake, after J. Hall, pers. comm. Oct. 2015).

- 2) Cross-sectional slices across medium-sized driftwood stems measuring 2–8 cm in diameter and 2 cm thick (Fig. 3a).
- 3) In situ shrinkage measurements on three timbers from an intact wooden anchor (Mazin A in Oron et al., 2008) found on the lake shore.

Table 1

List of examined wood samples and related information.

Sample	Wood species	Object	Age in YBP ^a	Origin	Sampling method ^b
DS8	<i>Ziziphus spina-christi</i>	Composite anchor (Mazine A) ^c	953	Dead Sea shore	1, 3
DS12	<i>Ziziphus spina-christi</i>	Carved wooden bowl	1647	Dead Sea shore	1
D7a	<i>Tamarix</i> (×5)	Driftwood (collected by diving in the lake)	136	Dead Sea shore	1, 2
D11	<i>Tamarix</i> (×5)	Drift wood (collected by diving in the lake)	855	Dead Sea shore	1
S10	<i>Tamarix</i> (×5)	Driftwood	667	Dead Sea shore	1
S11	<i>Tamarix</i> (×5)	Driftwood	1263	Dead Sea shore	1
S12	<i>Tamarix</i> (×5)	Driftwood	2580	Dead Sea shore	1
S19a	<i>Tamarix</i> (×5)	Driftwood	2745	Dead Sea shore	1–2
S20a	<i>Tamarix</i> (×5)	Driftwood	1271	Dead Sea shore	1–2
Tantura F	<i>Tamarix smyrnensis</i>	Frame	1239	Mediterranean wreck site	1–2
S14	<i>Populus euphratica</i>	Driftwood	124	Dead Sea shore	1
S15	<i>Populus euphratica</i>	Driftwood	852	Dead Sea shore	1
Reference 1	<i>Tamarix</i> (5)	Branch	Modern	Dead Sea basin	1
Reference 2	<i>Ziziphus spina-christi</i>	Branch	Modern	Dead Sea basin	1
Reference 3	<i>Populus euphratica</i>	Branch	Modern	Dead Sea basin	1

^a See Table 1 in Supplementary Online for additional radiocarbon dating information.^b 1 – Small section used for density (Db) maximum water content (MWC) and ash content analysis. 2 – Radial cross-section used for shrinkage measurements (β) and anti-shrinkage efficiency (ASE). 3 – In situ shrinkage measurements on shank and arms of composite anchor DS8.^c Oron et al. (2008).

2.4.1. Basic density (Db) and maximum water content (MWC)

Before taking measurements, wood samples from the Dead Sea were stored in Dead Sea lake water and Tantura F samples in tap water. To prevent possible biased water content and density (MWC, Db) values due to the high mineral content of the Dead Sea sample group, samples used for these analyses were first desalinated. Desalination was done by gradual dilution of the initial storage water with de-ionized water at 20% increments at regular time intervals. The process was monitored with a calibrated conductivity meter, and was considered completed when conductivity readings reached a constant value of $\leq 50 \mu\text{S}/\text{cm}$. In order to achieve maximum water content, samples were then placed in a vacuum chamber for 30 min at 30 kPa. This cycle was repeated twice. The samples were then weighed after careful blotting of the excess water from their surface. The weight (Ms) of each sample was measured five times on a calibrated analytical scale (accuracy 0.001 g), and the average value was calculated. The volume (Vs) of each sample was then determined by the water displacement method by the procedure

of Jensen and Gregory (2006: 554–557), using a wide-mouth 25 ml Hubbard Carmick pycnometer on the same analytical balance.

Following these measurements, samples were dried in an oven at $103 \pm 2 \text{ }^\circ\text{C}$ to a constant weight, and their oven-dry weight (Mo) recorded after cooling in a desiccator. The results were used for the calculation of basic density (Db), maximum water content (MWC) and related parameters.

2.4.2. Shrinkage

The initial small size of some of the samples used for the study limited the shrinkage measurements to few larger cut samples and to several in-situ measurements taken directly from three timbers of the intact wooden anchor (DS8). Measurements were made using stainless steel pins inserted into the wood across its radial (r), tangential (t), and when possible (only on anchor sample DS8), on the longitudinal plane (l). Measurements were taken at full saturation and after slow air-drying in a controlled environment at $20 \text{ }^\circ\text{C}$ and 50% relative humidity (RH). Three measurements were taken using digital calipers (accuracy

Table 2

Methods used for physical characterization of waterlogged wood samples.

Parameter	Abbreviations	Method
Maximum water content (%)	MWC	$\text{MWC} = 100 \times \frac{(Ms - Mo)}{Mo}$
Basic density of archaeological sample at MWC (g/cm^3)	Db	$\text{Db} = \frac{Ms}{Vs}$
Basic density of non-degraded (fresh) wood from the literature (g/cm^3)	Db1	Data from literature
Residual basic density (%)	RBD	$\text{RBD} = 100 \times \frac{Db}{Db1}$
Loss of wood substance (%)	LWS	$\text{LWS} = 100 \times \frac{(Db1 - Db)}{Db1}$
Linear shrinkage (%)	β	$\beta = 100 \times \frac{(l_0 - l_1)}{l_0}$
Cross sectional shrinkage (%)	β_{cs}	$\beta_{cs} = 100 \times \left[\frac{1 - (1 - \beta_t) \times (1 - \beta_r)}{100} \right]$
Anti-shrinkage efficiency (%)	ASE	$\text{ASE} (\%) = \frac{(\beta_{cs} - \beta_{cst})}{\beta_{cs}} \times 100$

Abbreviations

Ms	mass of waterlogged wood (g) at MWC
Mo	mass of oven-dry wood (g)
Vs	volume of sample (cm^3) at MWC
Ms	mass of waterlogged sample (g)
Mo	mass of oven-dry sample (g)
Ash Desl.	ash desalinated = ash content after desalination
l0	distance between pins in wet state at MWC
l1	distance between pins after drying
$\beta_t, \beta_r, \beta_l$	linear shrinkage in tangential, radial and longitudinal directions (%)
β_{cst}	cross-sectional shrinkage of desalinated samples (%)

Table 3
Physical and chemical properties of the study wood samples with reference data on non-degraded modern wood density and ash content.

Sample	MWC (%)	Db (g/cm ³)	Dbl (g/cm ³)	RBD (%)	LWS (%)	Ash (%)	Ash Desl. (%)	βt (%)	βr	βl	βcs	ASE (%)
DS8 (<i>Ziziphus spina-christi</i>)	134	0.591	0.650	91.0	9.0	44.8	3.5	0.4	−0.3	0.1	0.2	NA
DS12 (<i>Ziziphus spina-christi</i>)	72	0.747	0.650	114.9	−14.9	18.8	6.3	−	−	−	−	−
D7a (<i>Tamarix</i> [×5])	176	0.423	0.635	66.6	33.4	22.2	2.3	2.5	0.6	NA	3.1	93
D11 (<i>Tamarix</i> [×5])	166	0.453	0.635	71.4	28.6	34.4	2.6	−	−	−	−	−
S10 (<i>Tamarix</i> [×5])	130	0.521	0.635	82.1	17.9	31.1	1.8	−	−	−	−	−
S11 (<i>Tamarix</i> [×5])	211	0.370	0.635	58.2	41.8	50.1	2.6	−	−	−	−	−
S12 (<i>Tamarix</i> [×5])	189	0.393	0.635	61.9	38.1	37.9	2.4	−	−	−	−	−
S19a (<i>Tamarix</i> [×5])	161	0.445	0.635	70.1	29.9	25.4	3.0	−0.3	−0.5	NA	−0.8	103
S20a (<i>Tamarix</i> [×5])	209	0.370	0.635	58.3	41.7	23.2	1.7	4.6	0.9	NA	5.5	91
Tantura F (<i>Tamarix smyrnensis</i>)	854	0.108	0.635	17.1	82.9	NA	2.9	28.8	34.6	NA	53.4	NA
S14 (<i>Populus euphratica</i>)	198	0.387	0.505	76.6	23.4	37.4	8.4	−	−	−	−	−
S15 (<i>Populus euphratica</i>)	174	0.419	0.505	83.1	16.9	32.0	1.4	−	−	−	−	−
Reference 1 <i>Tamarix</i> (×5)	−	−	0.635	−	−	6.8	1.5	−	−	−	−	−
Reference 2 <i>Ziziphus spina-christi</i>	−	−	0.650	−	−	11.0	5.5	−	−	−	−	−
Reference 3 <i>Populus euphratica</i>	−	−	0.505	−	−	1.7	1.8	−	−	−	−	−
Wood species and Dbl value ^a (g/cm ³)				Cited sources								
<i>Populus euphratica</i>	0.505			Lamers (2008): 44								
<i>Tamarix</i> spp. (<i>smyrnensis</i> and <i>aphylla</i>)	0.635			Crivellaro et al. (2013): 553; Mantanis and Birbilis (2010), Table 2; Sadegh et al. (2012), Table 1.								
<i>Ziziphus spina-christi</i>	0.65			Crivellaro et al. (2013): 463; Familian et al. (2008), Table 3; Global Forest, 2005								

^a Average value based on data from cited sources.

0.02 mm at 50% RH) and the average values were used to calculate linear shrinkage (β) across the three planes (βr, βt, βl). The total average sums were used to calculate cross-sectional shrinkage (βcs).

In order to evaluate the impact of the high mineral content of the samples from the Dead Sea on their dimensional stability, a second set of samples was prepared from each of the cut samples (D7b S19b, S20b). Their soluble mineral content was then removed by desalination following the protocol described above. After desalination, the dimensional changes of the samples in the radial and tangential planes were measured as above. The differences in shrinkage rates between this set of samples and the mineral saturated wood were used for the calculation of anti-shrinkage efficiency (ASE).

2.5. Ash content analysis

Ash content was measured by the standard loss-on-ignition method (Soil and Plant Analysis Council, 1999). Un-desalinated wood samples (Ash) and desalinated samples (Ash desal.) were dried at 105 °C overnight and cooled in a desiccator. Samples were then weighed in pre-weighed crucibles on an analytical balance to the nearest 0.0001 g. They were then heated to 500 °C for 4 h in a muffle furnace, cooled in a desiccator, and weighed again to determine ash content.

2.6. FTIR ATR

Five sub-samples approximately 4 × 4 mm were removed from each initial designated sample with a scalpel. Each sub-sample was placed on the diamond attenuated total reflectance (ATR) accessory of a Thermo Scientific Nicolet iS 10 spectrometer. The inner surface of the sub-sample was placed on the ATR crystal. The pressure tower on top of the sampling plate applied a constant pressure on the sample to ensure good contact between the sample and the ATR crystal. The laboratory in which the measurements were performed was maintained at 65 ± 2% RH and 24 ± 1 °C. FTIR spectra were recorded at a spectrum resolution of 4 cm^{−1} between 650 cm^{−1} and 4000 cm^{−1}, and averaged from 32 scans. A background scan of a clean diamond crystal was acquired before scanning each sample. Smoothing (3rd order Savitzky-Golay filter with 51 points) was applied to each spectrum to minimize absorbance bands to ambient water vapor. Smoothing was followed by baseline correction using the procedure developed by Mazet et al. (2005) (with a second order asymmetric truncated quadratic function) and normalization with the Vector Normalization procedure used by Pizzo et al.

(2015):

$$S_n = \frac{S - S_{avg}}{\sum (S - S_{avg})^2}$$

where S is the original spectrum, S_{avg} is the spectrum mean, and S_n is the normalized spectrum. The sum is on the spectral range considered, in the present case the 700–1800 cm^{−1} interval. Finally, the spectra of the five sub-samples were averaged, and these average spectra were used for the analysis reported below.

3. Results and discussion

3.1. Wood species

The samples examined were identified as *Ziziphus spina christi* (*Ziziphus spina-christi* [Christ thorn; Jujube], *Tamarix* (×5) [Tamarisk with 5 sepals, 5 petals and 5 stamens in the flower], *Tamarix smyrnensis* [*Tamarix*] and *Populus euphratica* [Euphrates poplar]) (Table 1). Of these four species, only *Tamarix smyrnensis* is not native. It originates in Izmir and Antalya on the Turkish coast, and was used as hull construction timber for the Tantura F ship (see Liphshitz, 2012). The other three species are native to the Dead Sea region. They were used for the anchor and the carved wooden bowl found on the Dead Sea shore, and were identified amongst the driftwood located along the shore.

3.2. Micromorphological analysis

3.2.1. Findings

Sound modern wood was sectioned to compare its micromorphological characteristics with the various woods from the Dead Sea, and with the Tantura F sample. Transverse sections of two woods, *Tamarix* (×5) and *Ziziphus spina-christi* are shown in Fig. 6a, b. Wood from the anchor, sample DS8 (*Ziziphus spina-christi*), appeared sound, and its structural integrity was intact. Sections of wood from below the surface layer showed some occluded vessel elements, and in general, cells were free of cell wall degradation (Fig. 6c and d). Sections of wood near the surface of the wood showed some cells with altered morphology (Fig. 6e). Secondary walls in some fiber cells were slightly eroded, and others had detached secondary walls. The compound middle lamellae between cells were not affected, and most cells retained normal cell structure. The areas where cell wall alterations occurred were localized

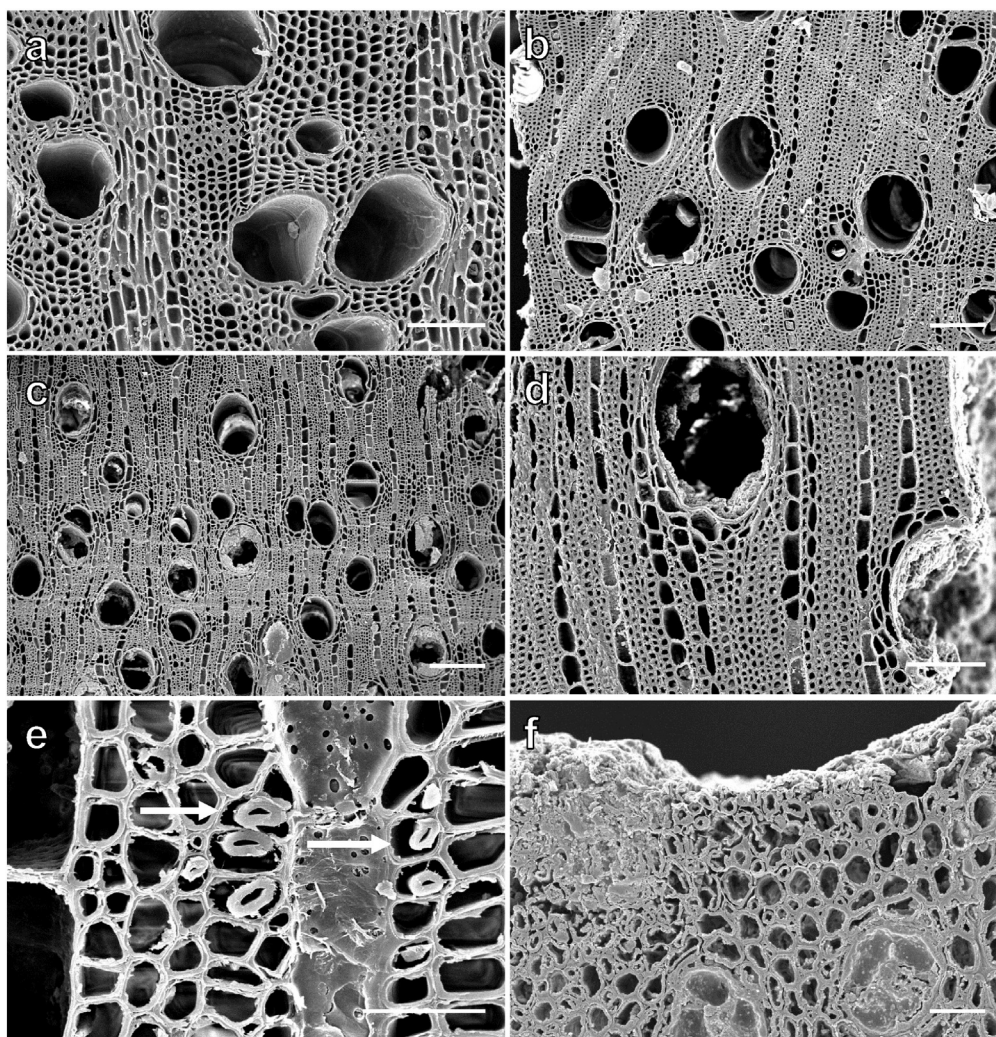


Fig. 6. Transverse sections of wood. Scanning electron micrographs of transverse sections of modern wood (a and b) from the Dead Sea Region, archaeological wood (c and d) and ancient driftwood (e). a, Sound *Tamarix* ($\times 5$) wood showing cell structure. Scale = 100 μm . b, Sound *Ziziphus spina-christi* wood. Scale = 100 μm . c, and d, *Ziziphus spina-christi* wood from anchor sample DS8, showing generally sound and intact wood cells. Some occlusions in vessel elements and cell walls are free of degradation. Scale = 200 μm [c] and 100 μm [d]. e, Areas of wood surface showing fibers with slightly eroded secondary walls, and cells with detached secondary cell wall layers (arrowed). Scale = 25 μm . f, Wood cells of *Tamarix* ($\times 5$) from sample D7 with heavily occluded vessels and fibers. Scale = 25 μm .

near the wood surface. Wood cells in Sample D7 (*Tamarix* ($\times 5$)) were heavily occluded (Fig. 6f). Salts and other substances filled vessel elements and coated the fiber cell walls. At the edge of this wood, cells were separated and defibrated. The compound middle lamellae between cells were degraded, and swollen secondary walls were detached from one another. This pattern of detached cells also occurred in wood at the outer surface of many other wood samples. More pronounced defibration was evident in sample S12 (*Tamarix* ($\times 5$), Fig. 7a and b), and large groups of cells were detached with no detectable compound middle lamellae remaining between cells. Cells at wood surfaces were defibrated and separated into individual strands of secondary wall material. Some samples, such as S14 (*Populus euphratica*), had large deposits of crystalline compounds within vessel elements and fiber cells, but did not display significant defibration or disruption of the wood cells (Fig. 7c). There was substantial degradation in wood from Sample S11 (*Tamarix* ($\times 5$), Fig. 7d), with large areas of eroded wood cells and voids. Large groups of cells remained unaltered between the degraded areas. Some large voids in the radial plane appeared to follow the ray parenchyma cells. This sample was thus a mixture of intact zones of cells, localized areas of defibrated cells, and relatively large voids containing remnants of degraded cell walls.

In contrast to the deterioration found in wood samples from the Dead Sea, the Tantura F samples showed extensive decay (*Tamarix*

smyrnensis, Fig. 7e). Cells appeared much degraded, and the remaining wood cells were greatly distorted during sample preparation and drying. Increased magnification showed wood cells with advanced stages of bacterial degradation (Fig. 7f). Some cells had secondary cell walls that were completely degraded, leaving only the compound middle lamellae; while others had swollen and very porous secondary walls.

3.2.2. Discussion

In certain environments, high concentrations of salts in wood can cause serious damage to wood. This occurs when wood absorbs moisture and salts from the surrounding environment, and evaporation causes salt to be deposited in the wood. Over time, without rainfall to wash out the salts, the salt concentrations can become exceedingly high. Archaeological wood found in dry deserts, and historical woods along coastal areas in Antarctica and the Arctic, have been found with severe wood defibration caused by high salt contents (Blanchette et al., 1994, 2002, 2008; Ortiz et al., 2014). This deterioration, however, is not caused by the physical formation of salt crystals in cell lumina. Although the process is not well understood, salts cause a chemical reaction that affects the compound middle lamellae between cells, causing secondary walls to separate. With time, the surface wood cells continue to defibrate, causing a white fibrous appearance and a slow corrosion of the wood. The rate and extent of deterioration apparently depends on

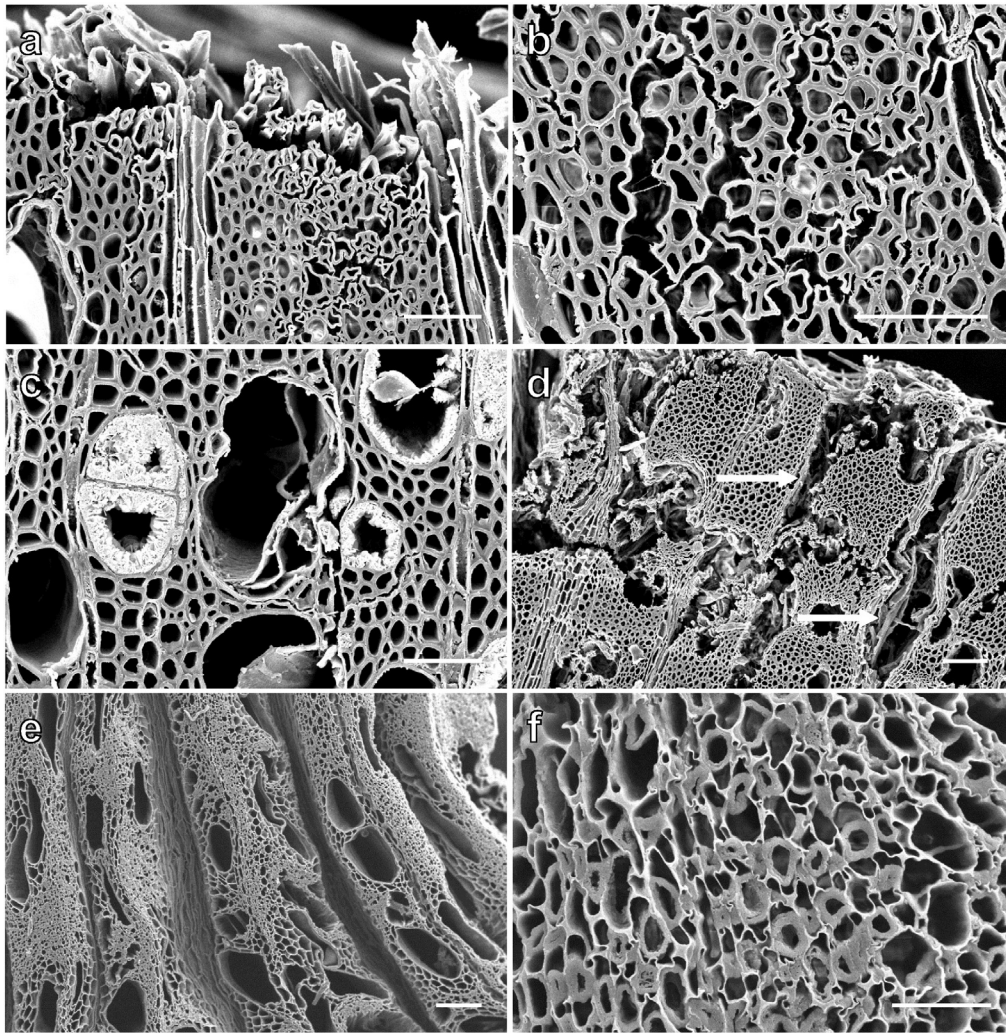


Fig. 7. Scanning electron micrographs of transverse sections. a to d. SEMs of transverse sections of ancient driftwood samples from the Dead Sea. a and b. Advanced defibration of wood cells from sample S12 showing the separation of the wood cells near the surface of the wood. The compound middle lamellae between cells were destroyed, causing the cells to separate and detach from one another. c. Wood section from sample S14 with large deposits of crystalline materials within vessel elements and fibers. d. Section showing degradation in sample S11 – eroded wood cells and voids. Defibrated cells in degraded areas, and large groups of unaltered cells between degraded zones. Some voids in the radial plane appear to follow ray parenchyma cells (arrows). e and f. Wood from the Tantara F shipwreck. Extensive degradation by bacteria in all wood cells with some secondary walls of fibers completely degraded, and others appearing swollen and porous. The compound middle lamellae remained intact and unaltered. Scale = 50 μm in a, b and c; 100 μm in d and e; 25 μm in f.

the environment. For example, wood only a few decades old may become extensively defibrated if it has a high salt content (Blanchette et al., 2002, 2004; Ortiz et al., 2014); while much older wood with high salt content in the Dead Sea region suffers limited attack. This may be due to the type of salts and the waterlogged condition of the wood. The latter prevents the occurrence of wet and dry cycles, which most probably accelerate this form of degradation.

The high contents of salts and other compounds in the wood found along the Dead Sea shore are probably responsible for inhibiting microbial degradation. There are very few environments where microbial decay does not take place when wood is found together with moisture. The Dead Sea appears to be one of these locations. In less salty sea water, such as the Mediterranean, archaeological wood is found with extensive microbial degradation. In this study, wood from the Tantara F showed an advanced stage of decay caused by bacterial degradation.

3.3. Physical analysis

3.3.1. Maximum water content

The maximum water content (MWC) values of the Dead Sea material range between 72% (DS12) and 211% (S11). A significantly higher MWC (854%) was measured in the Tantara F sample. This latter value

corresponds well with MWC data from other waterlogged shipwrecks in the Mediterranean (Capretti et al., 2008; Table 7; Pizzo et al., 2010; Table 2). A classification system proposed by Christensen (1970) and De Jong (1977), and commonly cited in the conservation literature, relates maximum water content to the degree of wood degradation. Plotting the research wood sample MWCs according to this classification system (Fig. 8) defines the Tantara F sample as Class I (400% and higher) – ‘highly degraded’ wood; while the Dead Sea samples are at the lower end of Class II (185%–400%) – ‘moderately degraded’ wood, ranging between 189% (S12) and 211% (S11); and Class III (less than 185%) – ‘non-degraded wood’, ranging between 72% (DS12) and 176% (D7a).

The relatively low MWC values of the Dead Sea samples indicate lower deterioration levels than the MWC data from the Mediterranean.

There seems to be no correlation between the age of the samples from the Dead Sea and their level of decay based on MWC values ($R^2 = 0.0077$) (see Fig. 1 in Supplementary online). For example, the MWC values of the two oldest samples in the group (S19a, 2745 YBP, MWC = 161% and S12, 2580 YBP, MWC = 189%) are not much different from the MWC values of the most recent samples (D7a, 136 YBP, MWC = 176% and S14, 124 YBP, MWC = 198%). This lack of correlation within the Dead Sea sample group may suggest the presence of micro-environments within the lake in which different rates of decay may

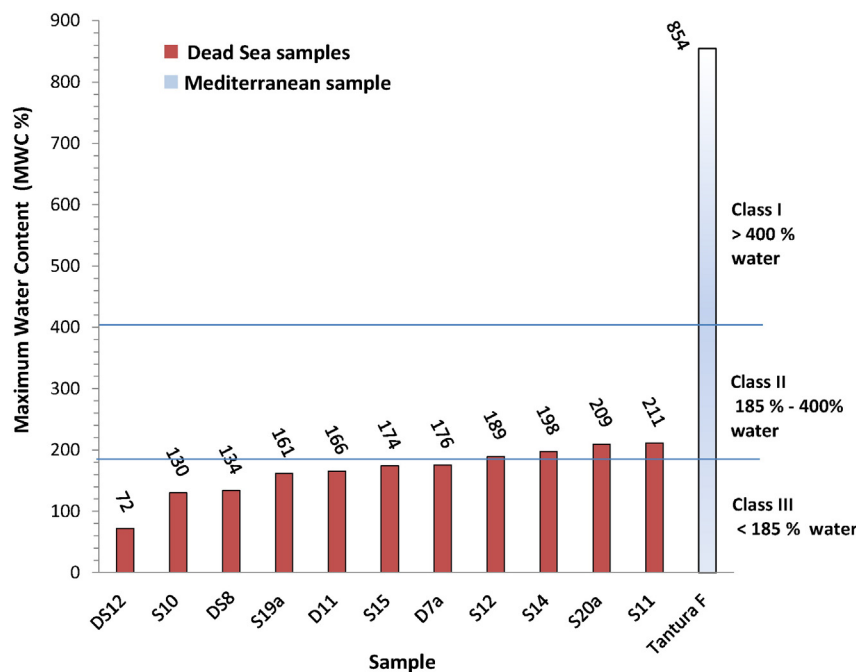


Fig. 8. Maximum water content of wood samples vs. Christensen and Dejong's wood degradation class system.

occur (Ionescu et al., 2012), or possibly variation in the pre-depositional conditions of some of the wood used in the study.

3.3.2. Density measurements

Basic density (Db) measurements quantify the degradation state of waterlogged wood. The amount of change or difference between the basic densities of the degraded wood and literature references of recent (modern) wood of the same species (Db1) is then expressed as residual basic density (RBD) and loss of wood substance (LWS). Table 3 shows that, with the exception of sample DS12, Db values are lower than the average values of their fresh wood counterpart (Db1). This suggests that various degrees of degradation have occurred in all the samples.

Db values of the Dead Sea samples range between 0.369 g/cm^3 (S11) and 0.747 g/cm^3 (DS12), whereas the Tantura F sample shows a significantly lower Db value (0.108 g/cm^3), indicating its advanced level of degradation. The highest basic density values amongst the Dead Sea samples occurred in *Ziziphus spina-christi*, which also has a higher basic density value when fresh (0.650 g/cm^3). Natural variations in wood density between different tree species and even within the same species, stemming from growth rates, position of sample within the tree and other factors (Schniewind, 1990: 90–91; Hacke et al., 2001; Westoby et al., 2002; Chave et al., 2006), mean that calculations based on average basic density are prone to some error. Nevertheless, it is likely that the values presented here for the archaeological wood vary from the actual basic density of non-degraded wood, due to varying levels of wood degradation. The level of material loss in each of the samples relative to the average basic density of non-degraded (fresh) wood is expressed as % RBD.

In practice, RBD should be less than 100%, and LWS should have a positive value. In some samples the basic density of archaeological wood was higher than the value for non-degraded wood, i.e. the RBD was higher than 100% (DS12). Thus the LWS values were negative. These values were not taken into consideration.

Residual basic density (RBD) values vary due to the level of degradation of each sample, but also because of the initial difference in the basic density between the different wood species. Using loss of wood substance (LWS) on the other hand allows a comparison of the percentage decay rates of different tree species. The highest loss of wood substance (the greatest decay) within the research group occurred in the sample

from the Mediterranean Tantura F (82.9%). the loss of wood substance of the research material from the Dead Sea (excluding DS12) is significantly lower, ranging from 9.0% (DS8) to 41.8% (S11), and averaging 28.1%.

As the deterioration of waterlogged wood proceeds, the loss of wood substance causes a drop in its basic density accompanied by increased absorption of water. These linked processes are shown by the strong correlation between MWC and Db values ($R^2 = 0.9151$) (see Fig. 2 in Supplementary online).

Sample DS12 – a carved wooden bowl fragment dated to the Late Roman period – has unusually high Db (0.747 g/cm^3) and low MWC (72%) values. These values, which indicate very low degradation levels, may point to a non-waterlogged origin for this object. This could be an eroding archaeological land site from which the bowl may have been washed onto the lakeshore; or a change in the physical properties of the wood caused during the production or use of this object.

3.3.3. Shrinkage

Loss of cell wall material – reflected in reduced density and increased water content – leads to a considerable loss of original strength in archaeological waterlogged wood. Upon drying such wood will thus shrink, warp and crack, depending on the level of material loss.

Shrinkage rates of a limited selection of wood samples were measured (Table 3 and Fig. 3b).

The cross-sectional shrinkage (β_{cs}), expressing the total of linear shrinkage, or expansion in some cases, of the Dead Sea samples after slow air-drying, is 2%. Radial (r) shrinkage within this group averages 0.2%; tangential (t) 1.8%; and longitudinal (l) 0.1%. Higher shrinkage rates in the tangential plane than in the radial and longitudinal planes are a common characteristic of fresh wood, and occur to varying degrees in archaeological waterlogged wood, as is the case here (De Jong, 1977: 298–299, Table 1; Stamm, 1977; Schniewind, 1990: 94–98). Shrinkage along the longitudinal plane in fresh and archaeological waterlogged wood is usually very small, and is often ignored. In the sample from the Dead Sea where such a measurement was possible (DS8), its value was 0.1%.

In general, the shrinkage rates of the air-dried samples from the Dead Sea are extremely low when compared to waterlogged wood finds from other marine environments. A good example of the latter is

the highly degraded Mediterranean sample from the Tantura F. In this sample, cross-sectional shrinkage (β_{cs}) is 53.4%, and the radial and tangential shrinkage are 34.6% and 28.8% respectively. While these values derive only from one sample, they are widely corroborated by data from other studies of waterlogged wood finds from marine sites (Schniwind, 1990: Table 4; Macchioni, 2003: Table 3).

The small number of samples available for shrinkage measurements shows that shrinkage rates, although minimal amongst the Dead Sea samples, increase with the increase of the degree of wood degradation indicated by the MWC samples (Fig. 9).

3.3.4. Ash content, mineral build-up and anti-shrinkage efficiency (ASE)

Whereas most sound woods have an ash content of less than 1 wt%, the ash content in waterlogged archaeological wood may be 10% or more (Grattan and Mathias, 1986; Fig. 9; Hoffmann, 1982: Table 2; Mikolajchuk et al., 1989: Table 1; Hedges, 1990: 137; Hoffmann and Jones, 1990: Table 2; Bettazzi et al., 2005: Tables 3–4; Babiński et al., 2014: Table 3).

At the Dead Sea, the mineral content of waterlogged wood is greatly increased by the high mineral content of the lake (ca. 30% dissolved salts), and is clearly visible in micromorphological examination (Figs. 6f, 7c). Massive mineral crusts also encapsulate many wooden objects (Fig. 4). The ash content analysis of the wood samples from the Dead Sea (Table 3) indicates an average mineral content (Ash) five times higher (32.5%) than that measured in the reference samples (6.5%).

Most of these minerals migrate into the wood during its submersion in the lake, as indicated by the ash content of samples D7a (22.2%) and D11 (34.4%); both collected during dives in the lake. Additional deposition of minerals probably takes place during the exposure of the wood on the shore, similarly to the mechanism reported above (3.2.2) in coastal regions of the Ross Sea in Antarctica and the high Arctic.

The dimensional stability of the finds from the Dead Sea afforded by the soluble minerals in the wood during drying may be expressed as anti-shrinkage efficiency (ASE). This measures the effect of a specific conservation treatment on the shrinkage of waterlogged wood (Grattan and Clarke, 1987: 197–198). The ASE was obtained by comparing the average air-dried shrinkage of the wood samples from the Dead Sea with that of a set of samples from which the soluble mineral content had been removed by gradual desalination down to an average ash content (Ash Desal. 3.3%) almost to the level of the desalinated reference samples (2.9%).

The differences in the shrinkage rates between the two sets of samples after slow drying are apparent visually (Fig. 3b) and through measurements of dimensions (Fig. 10). Average shrinkage rates were much higher in the desalinated samples than in the mineral-laden material: in

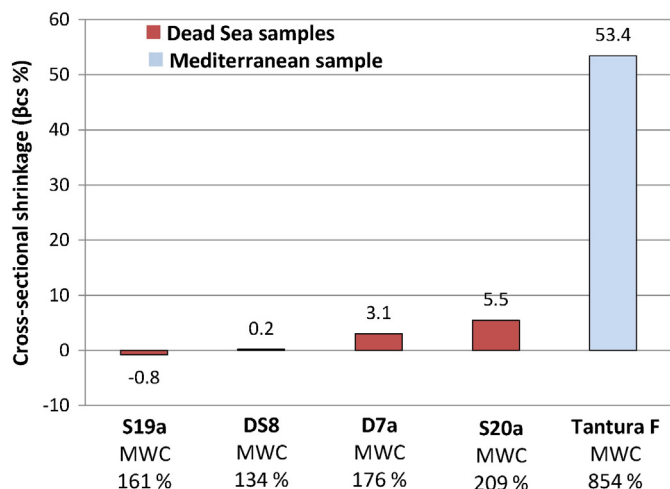


Fig. 9. Cross-sectional shrinkage of the wood samples after slow air-drying vs. MWC.

the radial plane – 25.0% against 0.4%; in the tangential plane – 28.9% against 2.2%; and in total average cross-sectional shrinkage – 44.8% against 2.6%. An average ASE value was 96%. This indicates that the soluble mineral content within these wood samples suppressed 96% of the shrinkage which would have been expected had it not been present in the wood.

It is generally agreed that a successful conservation treatment should attain a minimum ASE value of 75% (Morgos and Imazu, 1993: 289). For example, the ASE value measured on the Bremen Cog hull timbers after its prolonged PEG treatment was 92% (Hoffmann, 2001).

The high ASE values of the mineral saturated wood samples from the Dead Sea highlights the central role played by the mineral content of the finds on their dimensional stability upon drying.

3.4. FTIR ATR analysis

3.4.1. Dead Sea versus Mediterranean Sea

Fig. 11 shows the normalized average spectra of all the *Tamarix* samples. The 'modern' sample was dry, which explains the much lower absorbance in the 1600–1700 cm^{-1} range. Comparing the spectra of the 'modern' sample with that of the archaeological finds reveals the disappearance of the 1733 cm^{-1} and 1235 cm^{-1} bands in all archaeological spectra. These absorbance bands are associated with xylan C=O (Kuo et al., 1988; Bjarnestad and Dahlman, 2002; Chen et al., 2010; Lionetto et al., 2012). The absence of the 1733 cm^{-1} band in the spectra of archaeological finds was also reported by Pizzo et al. (2015). Comparison between the spectra of the Dead Sea finds and the spectrum of the Tantura F sample shows the relative decrease of all the bands associated with cellulose and polysaccharides (897, 1027, 1050, 1107, 1158 cm^{-1}) and the corresponding relative increase of all the absorbance bands associated with lignin (1120, 1230, 1266, 1327, 1460 cm^{-1}) (Petrou et al., 2009; Pizzo et al., 2013, 2015) in the latter. Lignin content relative to polysaccharides is a good indicator of the degree of bacterial attack, since bacteria predominantly decompose polysaccharides, so that the relative lignin content increases with the degree of bacterial attack (Gelbrich et al., 2008; Hoffmann et al., 1986; Troya et al., 1989a, 1989b; Kim, 1990; Blanchette et al., 1991). The results show that the Dead Sea environment greatly reduced microbial degradation of wood, compared to the more common kind of marine burial environment of the Tantura F sample. This observation is corroborated by the micromorphological analysis. In particular, other than xylan (1733 cm^{-1} and 1235 cm^{-1} bands), the polysaccharide content of the Dead Sea sample from 2597 BP (S19a) was virtually indistinguishable from that of the 'modern' sample.

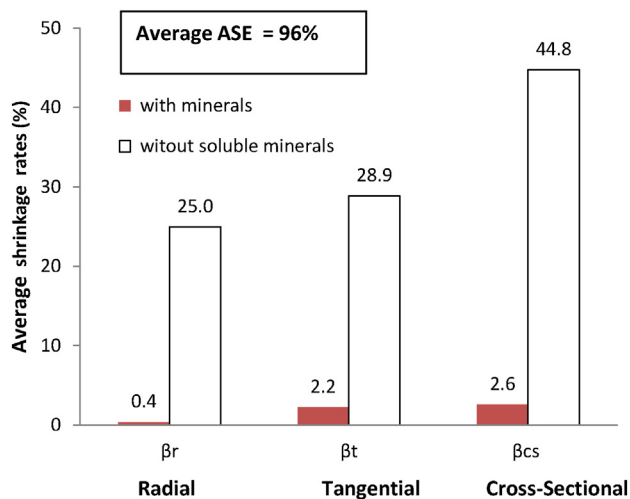


Fig. 10. Shrinkage. Average anti-shrinkage efficiency (ASE), and linear and cross-sectional shrinkage of wood samples after slow air-drying with and without soluble mineral content (measured at 50% RH).

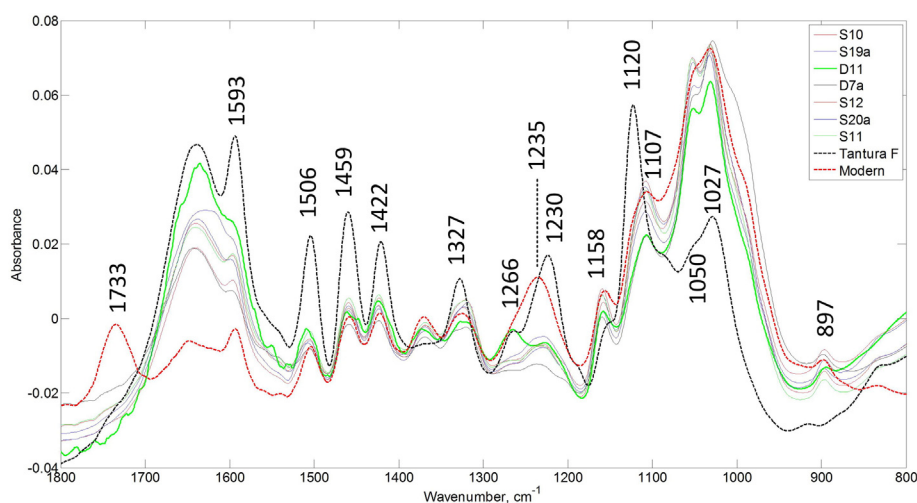


Fig. 11. Normalized average spectra of all *Tamarix* samples. 'Modern' corresponds to reference 1 (modern *Tamarix* ($\times 5$)). Tantara F corresponds to a Byzantine archaeological find from the Mediterranean Sea. All other spectra correspond to archaeological finds from the Dead Sea.

The change in the xylan shown by the ATR FTIR analysis is important in understanding the condition of the waterlogged wood. Xylan is a group of hemicelluloses found in plant cell walls. Along with lignin it fills the interstices between the cellulose microfibrils (Florian, 1987: 27–28). The chemical alterations of the hemicellulose affect the lignocellulose cell wall matrix, and are probably closely linked with the extreme shrinkage that characterizes degraded waterlogged wood (Schniewind, 1990: 95). This alteration may explain the separation of cells observed in the Dead Sea wood samples and its significant shrinkage after desalination.

3.4.2. Dead Sea – different wood types

Due to the limited number of samples, it is difficult to reach definite conclusions regarding differences between the various finds from the Dead Sea area. Fig. 12a shows the average spectra of all 11 finds.

In order to identify ranges in which the spectra of the various finds exhibited consistent significant differences, we applied principal component analysis (PCA) to all the individual spectra (rather than to the average spectra). PCA is a mathematical procedure for analyzing high-dimensional data such as mid-IR spectra (e.g. Jackson, 1991; Brereton, 2003). The information contained in the original data is condensed into a small number of 'scores', which are the projections of the original data onto new reference axes. Most of the information (variance) contained in the original data is reflected in the first few scores, and similarity/dissimilarity in the original data can be investigated by plotting these scores against each other and identifying score clusters.

The only spectral range found to give consistent results was 1160–1300 cm^{-1} . As shown in the Fig. 12a insert, absorbance in *Ziziphus spina-christi* (DS8 and DS12) is stronger at 1266 cm^{-1} than at 1230 cm^{-1} , while in the *Populus euphratica* spectra (S14 and S15) the two absorbances are similar. For *Tamarix* (D7a, D11, S10, S11, S12, S19a, S20a), the absorbance at 1230 cm^{-1} is stronger than at 1266 cm^{-1} , except for D11. This is verified by the three distinct clusters of PCA scores in the scatter plot in Fig. 12b. Although it would be tempting to associate the spectral differences with the wood type, this could not explain the results observed for D11. At this point, we cannot explain the observed differences, and further investigation using other measurement techniques is required.

4. Conclusions

Micromorphological, physical and chemical analyses showed less sign of biological and chemical degradation in waterlogged wood

samples from the Dead Sea than in similar material from less highly saline marine environments.

The increased shrinkage rates of the wood samples from the Dead Sea after their desalination are a result of the high mineral content of the Dead Sea, the latter acts not only as an inhibitor of wood biodegradation processes, but also as an important factor contributing to the physical stability of waterlogged wood finds from the lake during their exposure and subsequent drying.

The deposition of wooden cultural heritage material in the Dead Sea, and its subsequent exposure on shore, is a two-phase process.

In the first phase, starting at the submersion of the wood in the Dead Sea, all pre-burial biodegradation processes and new microbial colonization are halted by the hyper-saline water. Although little or no biological degradation seems to have occurred in this phase, some degradation did occur, possibly through non-biological chemical reactions. This degradation is indicated by the reduced Db values, loss of wood substance (LWS), increased MWC and shrinkage rates, as well as by the absence of bands associated with xylan from the ATR FTIR spectra. The latter may be linked to the separation of cells, observed by micromorphological examination, possibly through the chemical breakdown of the lignin-hemicellulose matrix. This phase is also characterized by the migration of lake minerals into the wood cells and lumens.

In the second phase, starting with the exposure of objects on shore, slow dehydration begins, and with it a gradual crystallization of the dissolved minerals within the cell walls and lumens. This process reduces or entirely prevents the shrinkage of the degraded wood as it dries. The small volume increase observed in some of the wood samples upon drying may be related to an increase in the volume of the minerals within the wood, due to their crystallization. This process seems to bring about chemical alteration of wood cells and internal cracks observed in the micromorphological analysis. Post-burial mechanical and chemical degradation processes may be continued by repeated wet and dry cycles on the lake shore, or due to uncontrolled environmental conditions in storage or display areas.

The degradation of waterlogged wood finds from the Dead Sea and the process by which they were impregnated by the lake minerals should be taken into account when they are retrieved, stored and conserved. Parameters, such as wood density and maximum water content, commonly used as guidelines in the planning of a specific conservation treatment of a waterlogged wood object, should be considered together with other data, such as the object's mineral content and storage environment. An attempt to wash the minerals out of waterlogged wood finds from the lake intentionally or accidentally by storing them in low

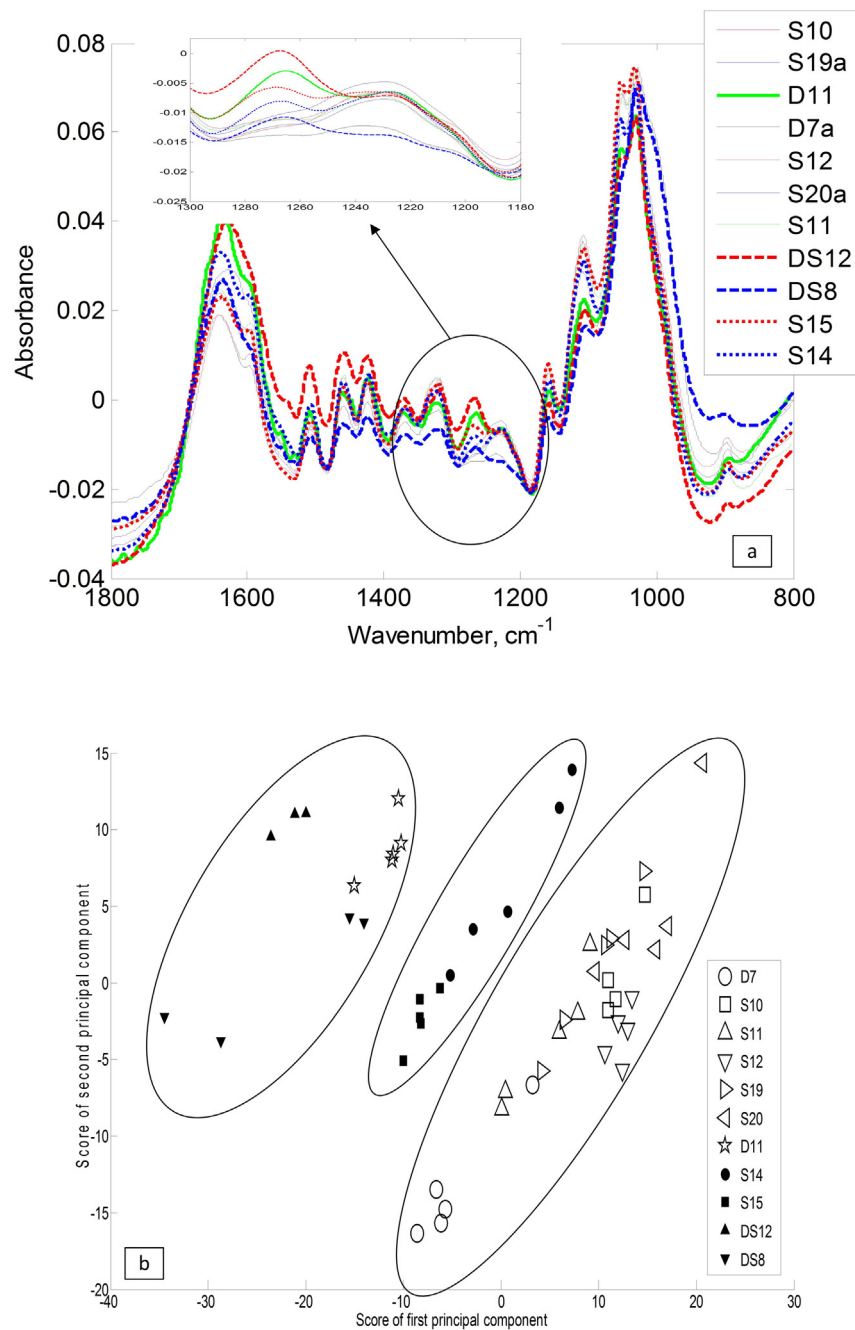


Fig. 12. Spectra. a) Average normalized spectra of all archaeological finds. Solid lines correspond to *Tamarix* samples, dashed lines correspond to *Populus* samples, and dotted lines correspond to *Ziziphus* samples (see Table 1 for details of each sample). The insert shows the 1100–1300 cm⁻¹ region in more detail. b) Scatter plot of the PCA scores of all the spectra. PCA was applied to the 1160–1300 cm⁻¹ interval.

salinity water – a common practice when dealing with newly retrieved marine finds – will remove the salts from the wood and eliminate its stabilizing properties. On the other hand, leaving the minerals in the wood may lead to gradual breakdown through mechanical and chemical processes driven by uncontrolled storage and display environments.

Acknowledgements

The study was supported by a Regional Research Grant of the Israeli Ministry of Science and Technology (grant no. 3-8422), and by a PhD scholarship from the Department of Geography and Environmental Studies at the University of Haifa. Funding for fieldwork has been generously provided over the years by the RPM Nautical

Foundation, the Institute of Nautical Archaeology at Texas A&M University, the Minerva Dead Sea Research Center at Tel Aviv University, and the Dead Sea and Arava Science Center. Samples from the Dead Sea were kindly collected during scuba diving by Danny Ionescu and Stefan Häusler, and from the Tantura F shipwreck by Yaacov Kahanov and Ofra Barkai. The authors also acknowledge Roe Shafir for laboratory assistance, Adi Eliyahu and Ulrike Rothenhäusler for preliminary analyses and Amit Gross for the ash content analyses. The authors thank Gideon Hadas co director of the Dead Sea Coastal Survey project, Naama Sukenik and the Israel Antiquities Authority for sampling permission and the survey permits, Nurgül Külah for library assistance and Baruch Rozen for his advice and invaluable comments. Finally thanks are due to the two reviewers, whose comments have undoubtedly improved this article.

Appendix A. Supplementary data

Supplementary data to this article can be found online at <http://dx.doi.org/10.1016/j.jasrep.2016.06.049>.

References

- Babiński, L., Izdebska-Mucha, D., Waliszewska, B., 2014. Evaluation of the state of preservation of waterlogged archaeological wood based on its physical properties: basic density vs. wood substance density. *J. Archaeol. Sci.* 46, 372–383.
- Barkai, O., Kahanov, Y., 2007. The Tantura F shipwreck, Israel. *Int. J. Naut. Archaeol.* 36 (1), 21–31.
- Barkai, R., Gopher, A., Weiner, J., 2007. Quarrying flint at Neolithic Ramat Tamar—an experiment. In: Astruc, L., Binder, D., Briois, F. (Eds.), *Systèmes Techniques et Communautés du Néolithique Précéramique au Proche-Orient. Actes du 5ème Colloque International Fréjus*, 2004, Antibes, pp. 25–32.
- Barkai, O., Kahanov, Y., Avissar, M., 2010. The Tantura F shipwreck: the ceramic material. *Levant* 42 (1), 88–101.
- Bettazzi, F., Giachi, G., Staccioli, G., Chimichi, S., Macchioni, N., 2005. Chemical and physical characterization of wood from shipwrecks discovered in the ancient harbour of Pisa (Tuscany—Italy). In: Hoffmann, P., Strætkvern, K., Spriggs, J.A., Gregory, D. (Eds.), *Proceedings of the 9th ICOM Group on Wet Organic Archaeological Materials Conference*, Copenhagen, 7–11 June 2004, pp. 127–143.
- Bjarnestad, S., Dahlman, O., 2002. Chemical compositions of hardwood and softwood pulps employing photoacoustic Fourier transform infrared spectroscopy in combination with partial least-squares analysis. *Anal. Chem.* 74 (22), 5851–5858.
- Björdal, C.G., 2012. Evaluation of microbial degradation of shipwrecks in the Baltic Sea. *Int. Biodeterior. Biodegrad.* 70, 126–140.
- Blanchette, R.A., Hofmann, P., 1994. Degradation processes in waterlogged archaeological wood. In: Hofmann, P. (Ed.), *Proceedings of the Fifth ICOM Group on Wet Organic Archaeological Materials Conference*, Portland, Maine, pp. 111–137.
- Blanchette, R.A., Iiyama, K., Abad, A.R., Cease, K.R., 1991. Ultrastructure of ancient buried wood from Japan. *Holzforchung* 45 (3), 161–168.
- Blanchette, R.A., Haight, J.E., Koestler, R.J., Hatchfield, P.B., Arnold, D., 1994. Assessment of deterioration in archaeological wood from Egypt. *American Institute for Conservation—J. Am. Inst. Conserv.* 33, 55–70.
- Blanchette, R.A., Held, B.W., Farrell, R.L., 2002. Defibrillation of wood in the expedition huts of Antarctica: an unusual deterioration process occurring in the polar environment. *Polar Rec.* 38 (207), 313–322.
- Blanchette, R.A., Held, B.W., Jurgens, J.A., Haight, J.E., 2004. Wood deterioration in Chacoan great houses of the southwestern United States. *Conserv. Manag. Archaeol. Sites* 6, 204–212.
- Blanchette, R.A., Held, B.W., Jurgens, J.A., 2008. Northumberland House, Fort Conger and the Peary Huts in the Canadian High Arctic: current condition and assessment of wood deterioration taking place. In: Barr, S., Chaplin, P. (Eds.), *Historical Polar Bases — Preservation and Management/ICOMOS Monuments and Sites No. XVII. International Polar Heritage Committee*, Oslo, Norway, p. 96.
- Bookman, R., Bartov, Y., Enzel, Y., Stein, M., 2006. Quaternary lake levels in the Dead Sea basin: two centuries of research. In: Enzel, Y., Agnon, A., Stein, M. (Eds.), *New Frontiers in Dead Sea Paleoenvironmental Research. Geological Society of America Special Paper Vol. no. 401*, pp. 155–170.
- Brereton, R.G., 2003. *Chemometrics: Data Analysis for the Laboratory and Chemical Plant*. John Wiley & Sons, University of Bristol, UK.
- Capretti, C., Macchioni, N., Pizzo, B., Galotta, G., Giachi, G., Giampaola, D., 2008. Characterisation of the waterlogged archaeological wood: the three Roman ships found in Naples (Italy). *Archaeometry* 50 (5), 855–876.
- Chave, R., Muller-Landau, H.C., Baker, T.R., Easdale, T.S.A., Steege, H.T., Webb, C.O., 2006. Regional and phylogenetic variation of wood density across 2456 neotropical tree species. *Ecol. Appl.* 16 (6), 2356–2367.
- Chen, H., Ferrari, C., Angiuli, M., Yao, J., Raspi, C., Bramanti, E., 2010. Qualitative and quantitative analysis of wood samples by Fourier transform infrared spectroscopy and multivariate analysis. *Carbohydrate Polymers* 82 (3), 772–778.
- Christensen, B.B., 1970. *Conservation of Waterlogged Wood in the National Museum of Denmark*. National Museum of Denmark, Copenhagen.
- Crivellaro, A., Schweingruber, F.H., Christodoulou, C.S., Papachristophorou, T., Tsintides, T., Da Ros, A., 2013. *Atlas of Wood, Bark and Pith Anatomy of Eastern Mediterranean Trees and Shrubs: With a Special Focus on Cyprus*. Springer Science + Business Media.
- De Jong, J., 1977. *Conservation techniques of Old waterlogged wood from shipwrecks found in the Netherlands*. In: Walters, A.H. (Ed.), *Biodeterioration Investigation Techniques*. Applied Science Publishers, London, pp. 295–338.
- Fahn, A., Werker, E., Baas, P., 1986. *Wood Anatomy and Identification of Trees and Shrubs from Israel and Adjacent Regions*. Israel Academy of Sciences and Humanities, Jerusalem.
- Familian, H., Kharazipour, A., Hosseinkhani, H., 2008. Investigation on the anatomical, physical, and chemical characteristics of *Ziziphus spina-christi*, *Z. lotus*, *Z. mauritiana* and *Z. nummularia*. In: Kharazipour, A.R., Schöpfer, C., Müller, C. (Eds.), *In Review of Forests, Wood Products and Wood Biotechnology of Iran and Germany — Part II. Universitätsdrucke Göttingen*, pp. 85–99.
- Florian, M.-L.E., 1987. In: Pearson, C. (Ed.), *Deterioration of Organic Materials Other than Wood/Conservation of Marine Archaeological Objects*. Butterworths, London, Boston, pp. 21–54.
- Gelbrich, J., Mai, C., Militz, H., 2008. Chemical changes in wood degraded by bacteria. *Int. Biodeterior. Biodegrad.* 61, 24–32.
- Gichon, M., 2000. *Industry*. In: Fischer, M., Gichon, M., Tal, O. (Eds.), *En Boqeq: Excavation in an Oasis on the Dead Sea/The Officina vol. II. Philipp von Zabern, Mainz am Rhein*, pp. 93–102.
- Global Forest, 2005. *Global Forest Resources assessment country reports United Arab Emirates, FRA 2005/114 Rome*.
- Grattan, D.W., Clarke, R.W., 1987. In: Pearson, C. (Ed.), *Conservation of Waterlogged Wood/Conservation of Marine Archaeological Objects*. Butterworths, London, Boston, pp. 164–206.
- Grattan, D.W., Mathias, C., 1986. Analysis of waterlogged wood: the value of chemical analysis and other simple methods in evaluating condition. *Somerset Levels Pap.* 12, 6–12.
- Hacke, U.G., Sperry, J.S., Pockman, W.T., Davis, S.D., McCulloh, K.A., 2001. Trends in wood density and structure are linked to prevention of xylem implosion by negative pressure. *Oecologia* 126, 457–461.
- Hadas, G., 1992. Stone anchors from the Dead Sea. *Atiqot* 21, 55–57.
- Hadas, G., 1993. A stone anchor from the Dead Sea. *Int. J. Naut. Archaeol.* 22, 89–90.
- Hadas, G., Liphshitz, N., Bonani, G., 2005. Two ancient wooden anchors from Ein Gedi on the Dead Sea, Israel. *Int. J. Naut. Archaeol.* 34, 299–307.
- Hedges, J.L., 1990. *The chemistry of archaeological wood*. In: Rowell, R.M., Barbour, J. (Eds.), *Archaeological Wood; Properties, Chemistry and Preservation*. American Chemical Society, Washington DC, pp. 111–140.
- Hirschfeld, Y., 2006. The archaeology of the Dead Sea Valley in the Late Hellenistic and Early Roman periods. In: Enzel, Y., Agnon, A., Stein, M. (Eds.), *New Frontiers in Dead Sea Paleoenvironmental Research. Geological Society of America Special Paper Vol. no. 401*, pp. 215–229.
- Hoffmann, P., 1982. Chemical wood analysis as a means of characterizing archaeological wood. In: Grattan, D.W., McCawley, J.C. (Eds.), *Proceedings of the ICOM Waterlogged Wood Working Group Conference, 15–18th September 1981*. Canadian Conservation Institute. International Council of Museums (ICOM), Committee for Conservation, Waterlogged Wood Working Group, pp. 73–84.
- Hoffmann, P., 2001. To be and to continue being a cog: the conservation of the Bremen cog of 1380. *Int. J. Naut. Archaeol.* 30 (1), 129–140.
- Hoffmann, P., Jones, M.A., 1990. Structure and degradation process for waterlogged archaeological wood. In: Rowell, R.M., Barbour, J. (Eds.), *Archaeological Wood; Properties, Chemistry and Preservation*. American Chemical Society, Washington D.C., pp. 35–65.
- Hoffmann, P., Peek, R.-D., Puls, J., Schwab, E., 1986. *Das Holz der Archaeologen: Untersuchungen an 1600 Jahren wassergesättigten Eichenhölzern der "Mainzer Roemerschiffe"*. Holz als Roh- und Werkstoff Vol. 44, pp. 241–247.
- Ionescu, D., Siebert, C., Polerecky, L., Munwes, Y.Y., Lott, C., Häusler, S., de Beer, D., 2012. Microbial and chemical characterization of underwater fresh water springs in the Dead Sea. *PLoS One* 7 (6), e38319.
- Jackson, J.E., 1991. *A User's Guide to Principal Components*. John Wiley & Sons, New York.
- Jensen, P., Gregory, D.J., 2006. Selected physical parameters to characterize the state of preservation of waterlogged archaeological wood: a practical guide for their determination. *J. Archaeol. Sci.* 33, 551–559.
- Kim, Y.S., 1990. Chemical characteristics of waterlogged archaeological wood. *Holzforchung* 44 (3), 169–172.
- Klein, C., 1982. Morphological evidence of lake level changes, western shore of the Dead Sea. *Israel Journal of Earth Sciences*—>|sr. *J. Earth Sci.* 31, 67–94.
- Kuo, M.L., McClelland, J.F., Luo, S., Chien, P.L., Walker, R.D., Hse, C.Y., 1988. Applications of infrared photo-acoustic spectroscopy for wood samples. *Wood Fiber Sci.* 20, 132–145.
- Lamers, J.P.A., 2008. Fuel wood production in the degraded agricultural areas of the Aral Sea Basin, Uzbekistan. *Bois For. Trop.* 297, 43–53.
- Lionetto, F., Del Sole, R., Cannoletta, D., Vasapollo, G., Maffezzoli, A., 2012. Monitoring wood degradation during weathering by cellulose crystallinity. *Materials* 5 (10), 1910–1922.
- Liphshitz, N., 2012. Dendroarchaeological studies of shipwrecks along the Mediterranean coast of Israel. In: Efe, R., Ozturk, M., Ghazanfar, S. (Eds.), *Environment and Ecology in the Mediterranean Region*. Cambridge Scholars Publishing, pp. 1–12.
- Macchioni, N., 2003. Physical characteristics of the wood from the excavations of the ancient port of Pisa. *J. Cult. Herit.* 4 (2), 85–89.
- Mantanis, G.I., Birbilis, D., 2010. Physical and mechanical properties of Athel wood (*Tamarix aphylla*). *Suleyman Demirel Univ. (SDU) — For. Fac. J. A* (2), 82–87.
- Mazet, V., Carteret, C., Brie, D., Idier, J., Humbert, B., 2005. Background removal from spectra by designing and minimizing a non-quadratic cost function. *Chemom. Intell. Lab. Syst.* 76 (2), 121–133.
- Mikolajchuk, E.A., Gerassimova, N.G., Leonovich, A.A., Obolenskaya, A.V., Levdiik, I.Y., Kazanskaya, S.Y., 1989. Examination of waterlogged archaeological oak wood. *Conservation of Wet Wood and Metal: Proceedings of the ICOM Conservation Working Groups on Wet Organic Archaeological Materials and Metals*. International Council of Museums, pp. 95–107.
- Morgos, A., Imazu, S., 1993. Comparing conservation methods for waterlogged wood using sucrose, mannitol and their mixture. *Proceedings of the 5th ICOM Group on Wet Organic Archaeological Materials Conference, Portland 1993*, pp. 287–299.
- Nissenbaum, A., 1993. *The Dead Sea — an economic resource for 10,000 years*. Saline Lakes 5, 127–141.
- Oron, A., Hadas, G., Liphshitz, N., Bonani, G., 2008. A new type of composite anchor dated to the Fatimid-Crusader Period from the Dead Sea, Israel. *Int. J. Naut. Archaeol.* 37, 295–301.
- Oron, A., Galili, E., Hadas, G., Klein, M., 2015a. Two artificial anchorages off the northern shore of the Dead Sea: a specific feature of an ancient maritime cultural landscape. *Int. J. Naut. Archaeol.* 44, 81–94.
- Oron, A., Galili, E., Hadas, G., Klein, M., 2015b. Early maritime activity on the Dead Sea: bitumen harvesting and the possible use of reed watercraft. *J. Marit. Archaeol.* 10 (1), 65–88.

- Ortiz, R., Navarrete, H., Navarrete, J., Párragac, M., Carrasco, I., de la Vegac, E., Ortiz, M., Herrera, P., Blanchette, R.A., 2014. Deterioration, decay and identification of fungi isolated from wooden structures at the Humberstone and Santa Laura saltpeter works: a world heritage site in Chile. *Int. Biodeterior. Biodegrad.* 86, 309–316.
- Petrou, M., Edwards, H.G., Janaway, R.C., Thompson, G.B., Wilson, A.S., 2009. Fourier-transform Raman spectroscopic study of a Neolithic waterlogged wood assemblage. *Anal. Bioanal. Chem.* 395 (7), 2131–2138.
- Pizzo, B., Giachi, G., Fiorentino, L., 2010. Evaluation of the applicability of conventional methods for the chemical characterization of waterlogged archaeological wood. *Archaeometry* 52, 656–667.
- Pizzo, B., Pecoraro, E., Macchioni, N., 2013. A new method to quantitatively evaluate the chemical composition of waterlogged wood by means of attenuated total reflectance Fourier transform infrared (ATR FT-IR) measurements carried out on wet material. *Appl. Spectrosc.* 67 (5), 553–562.
- Pizzo, B., Pecoraro, E., Alves, A., Macchioni, N., Rodrigues, J.C., 2015. Quantitative evaluation by attenuated total reflectance infrared (ATR-FTIR) spectroscopy of the chemical composition of decayed wood preserved in waterlogged conditions. *Talanta* 131, 14–20.
- Recchi, A., Gopher, A., 2002. Birds and humans in the Holocene: the case of Qumran Cave 24 (Dead Sea, Israel). *Acta Zool. Cracov.* 45, 139–150.
- Sadegh, A.N., Kiaei, M., Samariha, A., 2012. Experimental characterization of shrinkage and density of *Tamarix aphylla* wood. *Cellul. Chem. Technol.* 46, 369–373.
- Schaub, T., Chesson, M.S., 2007. Life in the earliest walled towns on the Dead Sea plain: Bab edh-Dhra' and an-Numayra. In: Levy, T.E., Daviau, P.M.M., Younker, R.W., Shaer, M. (Eds.), *Crossing Jordan: North American Contributions to the Archaeology of Jordan*. Equinox, London, pp. 245–252.
- Schniewind, A.P., 1990. Physical and mechanical properties of archaeological wood. In: Rowell, R.M., Barbour, R.J. (Eds.), *Archaeological Wood. Properties, Chemistry, and Preservation*. American Chemical Society, Washington DC, pp. 87–109.
- Schweingruber, F.H., 1990. *Anatomy of European Woods*. Haupt, Bern and Stuttgart.
- Schyle, D., 2007. Ramat Tamar and Mezad Mazal, the early Neolithic economy of mining and production of bifacials southwest of the Dead Sea. *Bibliotheca Neolithica Asiae Meridionalis et Occidentalis, Ex Oriente, Berlin*.
- Soil and Plant Analysis Council, 1999. *Soil Analysis, Handbook of Reference Methods*. CRC Press, Boca Raton, Florida, USA.
- Stamm, A.J., 1977. Dimensional changes of wood and their control. *ACS Symposium Series*. American Chemical Society, pp. 115–140.
- Taute, W., 1994. Pre-Pottery neolithic flint mining and flint workshop activities southwest of the Dead Sea, Israel (Ramat Tamar and Mesad Mazzal). In: Gebel, H.G., Kozłowski, S.K. (Eds.), *Neolithic Chipped Stone Industries of the Fertile Crescent, Ex Oriente, Berlin*, pp. 495–510.
- Troya, M.T., Escorial, M.C., Garcia, J., Cabañas, A., 1989a. Study of the degradation caused by microorganisms in *Pinus* spp. *Waterlogged Wood, IRG/WP/1411*. International Research Group on Wood Preservation, Stockholm.
- Troya, M.T., Garcia, A., Pozuelo, J.M., Navarrete, A., Cabañas, A., 1989b. Contribution to Study of the Degradation Caused in *Pinus* spp. Conference: 22–26/5/1989, Lappeenranta, Finland.
- Vardi, J., Cohen-Sasson, E., 2012. Har-Parsa: a large-scale larnite quarry and bifacial tool production site in the Judean Desert, Israel. *Antiquity* 86, 332.
- Westoby, M., Falster, D.S., Moles, A.T., Vesk, P.A., Wright, I.J., 2002. Plant ecological strategies: some leading dimensions of variation between species. *Annu. Rev. Ecol. Syst.* 33, 125–159.
- Zohary, M., 1962. *Plant Life of Palestine*. Ronald Press, New York.